Proceedings of the Czech–Japanese Seminar in Applied Mathematics 2006
Czech Technical University in Prague, September 14-17, 2006
pp. 185–192

NUMERICAL SOLUTION OF A FLOW OVER AN OBSTACLE

KATEŘINA SEINEROVÁ[1]

Abstract. This paper deals with a numerical solution of a viscous flow over a two-dimensional hill. The mathematical model is based on a system of Navier-Stokes equations for an incompressible flow. Space discretization is done by a central finite difference method, time discretization by a multistage Runge-Kutta method. To compute pressure in time, artificial compressibility method and time-marching method are used. Several numerical results of flows over a hill are presented.

Key words. Newton boundary conditions, Stefan-Bolzman law, heat conduction in buildings.

AMS subject classifications. 35K60, 35K65

1. Introduction. Flows over topography have attracted a great interest from not only fluid mechanics but also engineering in a variety of fields. We consider two-dimensional internal waves excited topographically in stably stratified flows in the atmospheric boundary layer (ABL) and in the channel of finite depth. Under these conditions, the fluid layer is bounded above by a horizontal rigid lid and below by a two-dimensional surface-mounted obstacle.

2. Solved Problems. System 1 - Flow over a hill in the Atmospheric Boundary Layer is described by the model which is based on Navier-Stokes equations for an incompressible flow. Governing equations modified according to the method of artificial compressibility can be recast in a conservative, non-dimensional and vector form.

$$\widetilde{R}W_t + F_x + G_y = \frac{\widetilde{R}}{Re}(W_{xx} + W_{yy}), \tag{2.1}$$

where $W = (p, u, v)^T$ is the vector of unknowns; p is the pressure, $(u, v)^T$ is the velocity vector. $Re = \frac{U_\infty L}{\eta/\rho} = \frac{U_\infty L}{\nu}$ is Reynolds number, $\widetilde{R} = diag(0, 1, 1)$. The terms F, G denote the inviscid fluxes and are defined by

$$F = (u, u^2 + p, uv)^T, \; G = (v, uv, v^2 + p)^T.$$

The flow is investigated in a 2D spatial domain as shown in Fig. 2.1. **Boundary conditions** for this case are set as follows:

a) inflow: $u = 1, v = 0$, extrapolated pressure $\frac{\partial p}{\partial x} = 0$,

b) outflow: $\frac{\partial u}{\partial x} = 0$, $\frac{\partial v}{\partial x} = 0$,extrapolated pressure $\frac{\partial p}{\partial x} = 0$,

c) upper boundary: $\frac{\partial u}{\partial y} = 0, v = 0$, extrapolated pressure $\frac{\partial p}{\partial y} = 0$,

d) bottom: $u = 0, v = 0$, extrapolated pressure: $\frac{\partial p}{\partial y} = 0$.

System 2 - Flows over a hill in a channel of finite depth (Stratification). This problem is described by a system of Navier-Stokes equations similar to the previous problem (2.1). Nevertheless, in this problem the density ρ is computed, together with the velocity (u_1, u_2) and the pressure p, ρ' is the density perturbation, $\varrho = \varrho_0 + \varrho'$,

[1]Department of Mathematics, Faculty of Nuclear Sciences and Physical Engineering, Czech Technical University in Prague.

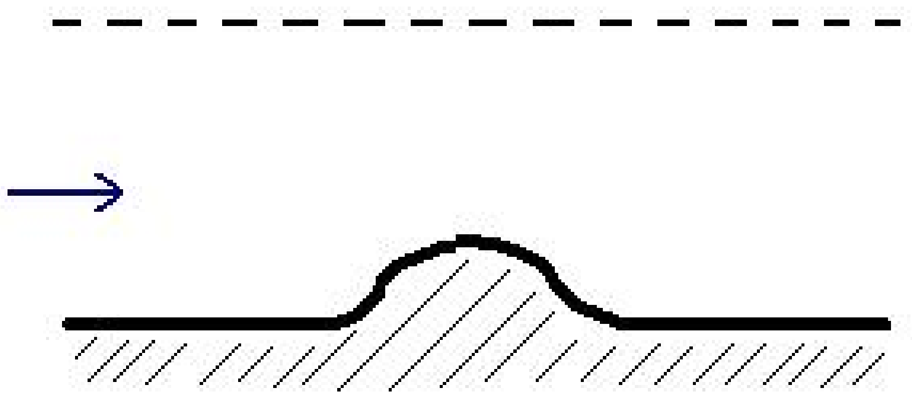

Fig. 2.1. *Spatial domain in the atmospheric boundary layer*

where ϱ_0 is the reference density. Boundary conditions are modified according to [1] by solving a similar problem.

$$
\begin{aligned}
\frac{\partial u_j}{\partial x_j} &= 0,\\
\frac{\partial u_i}{\partial t} + u_j \frac{\partial u_i}{\partial x_j} &= -\frac{\partial p}{\partial x_j} + \frac{1}{Re}\frac{\partial^2 u_i}{\partial x_j^2} - \frac{\rho \delta_{i2}}{Fr^2}, i = 1, 2,\\
\frac{\partial \rho'}{\partial t} + u_j \frac{\partial \rho'}{\partial x_j} &= u_3,
\end{aligned}
\tag{2.2}
$$

where Fr denotes the Froud number, and δ_{ij} is the Kronecker delta.

The flow is investigated in a 2D spatial domain as shown in Fig. 2.2. **Boundary conditions** for this case are set as follows:

a) inflow: $u_1 = 1, u_2 = 0$, extrapolated pressure $\frac{\partial p}{\partial x_1} = 0$, $p_0 = 0.5$, $\rho' = 0$,

b) outflow: $\frac{\partial u_1}{\partial x_1} = 0$, $\frac{\partial u_2}{\partial x_1} = 0$, $\frac{\partial \rho'}{\partial x_1} = 0$, extrapolation $\frac{\partial p}{\partial x_1} = 0$, $\frac{\partial \rho'}{\partial x_1} = 0$,

c) upper boundary: $\frac{\partial u_1}{\partial x_2} = 0, u_2 = 0$, extrapolated pressure: $\frac{\partial p}{\partial x_2} = 0$, $\rho' = 0$,

d) bottom part: except of the hill - the free-slip conditions are applied $u_2 = 0$, $\frac{\partial p}{\partial x_2} = 0$, $\frac{\partial u_1}{\partial x_2} = 0$, $\rho' = 0$;
on the hill surface - non-slip condition $u_1 = 0$, $u_2 = 0$, extrapolation: $\frac{\partial p}{\partial x_2} = 0$, $\frac{\partial \rho'}{\partial x_2} = 0$ are used.

3. Numerical Solution. To discretize the governing system of equations in space, a non-orthogonal structured boundary following the grid is constructed. Grid layers form an orthogonal system; the non-orthogonality is introduced to the grid by the curved terrain profile as shown in Fig 3.1. The **finite-difference** discretization is developed using a Taylor expansion for derivatives as follows.

a) Approximation of the 1st derivative in orthogonal grid is obtained

$$
\frac{\partial U}{\partial x} \sim \frac{1}{2}\left(\frac{U_{i+1} - U_i}{x_{i+1} - x_i} + \frac{U_i - U_{i-1}}{x_i - x_{i-1}}\right).
$$

Fig. 2.2. *Spatial domain in the channel*

b) The coordinate system is transformed and the derivative approximation is obtained:

$$D_x U_{ij} = \frac{U_{i+1,j} - U_{i-1,j}}{2\triangle s.\cos\alpha} - \frac{\sin\alpha(U_{i,j+1} - U_{i,j-1})}{2.\triangle y\cos\alpha}, \alpha = \frac{\alpha^- + \alpha^+}{2}.$$

c) Approximation of the 2nd derivative in orthogonal grid is obtained:

$$\frac{\partial^2 U}{\partial x^2} \sim \frac{2}{x_{i+1} - x_{i-1}}\left(\frac{U_{i+1} - U_i}{x_{i+1} - x_i} - ... - \frac{U_i - U_{i-1}}{x_i - x_{i-1}}\right).$$

d) The coordinate system is transformed and the second derivative approximation is obtained:

$$\begin{aligned}
D_{xx} U_{ij} = &\frac{U_{i+1,j} - 2U_{ij} + U_{i-1,j}}{(\triangle s.\cos\alpha)^2} - ...\\
&... - \frac{2\sin\alpha(U_{i+1,j+1} - U_{i+1,j-1} - U_{i-1,j+1} + U_{i-1,j-1})}{4.\triangle s.\triangle y.\cos^2\alpha}\\
&+ \frac{\sin^2\alpha(U_{i,j+1} - 2U_{ij} + U_{i,j-1})}{(\triangle y.\cos\alpha)^2} + ...\\
&... + \frac{U_{i+1,j} - U_{i-1,j}}{4.\triangle s^2.\cos\alpha}\left(\frac{1}{\cos\alpha_i^+} - \frac{1}{\cos\alpha_i^-}\right) - \frac{\sin\alpha(U_{i+1,j} - U_{i-1,j})}{4.\triangle s.\triangle y.\cos\alpha}\left(\frac{1}{\cos\alpha_j^+} - \frac{1}{\cos\alpha_j^-}\right) - ...\\
&... - \frac{U_{i,j+1} - U_{i,j-1}}{4.\triangle y.\triangle s.\cos\alpha}\left(\frac{\sin\alpha_i^+}{\cos\alpha_i^+} - \frac{\sin\alpha_i^-}{\cos\alpha_i^-}\right) + \frac{\sin\alpha(U_{i,j+1} - U_{i,j-1})}{4.\cos\alpha.(\triangle y)^2}\left(\frac{\sin\alpha_j^+}{\cos\alpha_j^+} - \frac{\sin\alpha_j^-}{\cos\alpha_j^-}\right).
\end{aligned}$$

For the time discretization, the 3-stage explicit **Runge-Kutta method** is used, which is designed for treatment of the problems (2.1-2.2) - see [4]. We denote $W = (p, u, v)^T$ in case of (2.1), or $W = (p, u, v, \rho')^T$ in case of (2.2) and consider the following scheme:

$$\begin{aligned}
W_{ij}^{(0)} &= W_{ij}^n,\\
W_{ij}^{(m)} &= W_{ij}^{(0)} - \alpha_m \triangle t R W_{ij}^m,\ m = 1, 2, 3,\\
W_{ij}^{n+1} &= W_{ij}^{(3)},
\end{aligned}$$

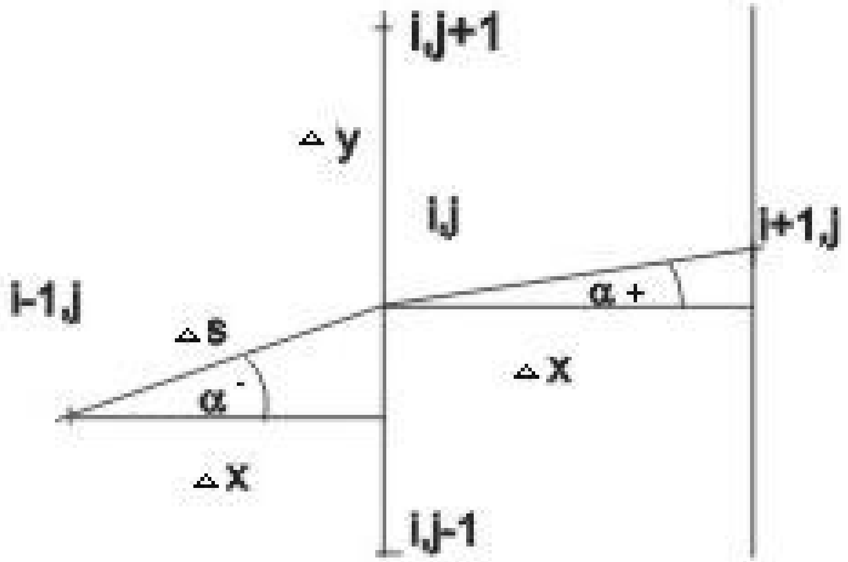

FIG. 3.1. *Transformation of coordinates along the hill*

where

$$RW = \frac{\partial F}{\partial x} + \frac{\partial G}{\partial y} - \frac{\widetilde{R}}{Re}(\triangle W).$$

For the values of the constants α_m, the reader is refered to [4].

Artificial compressibility and time-marching method. The solution procedure used in our method to resolve pressure is based on the so-called artificial compressibility method. This requires to add the time derivative of the pressure to the continuity equation, so the equation $\frac{\partial u_j}{\partial x_j} = 0$ transforms into $\frac{\partial p}{\partial t} + \frac{\partial u_j}{\partial x_j} = 0$. For an expected steady-state solution, this method is correct.

The governing system is then solved by a time-marching method. The governing system of equations is solved in the computational domain under stationary boundary conditions for $t \to \infty$ (t is artificial time) to obtained the expected steady-state solution for the pressure and the velocity components.

4. Numerical Results. In this section, results of the numerical solution of a flow over a hill are presented, which were obtained using a 250×100 grid with $Re = 2000$. The top of the hill is in the height of 1/10 of the computational domain height. These results were obtained from both numerical models - flows in atmospherical boundary layer and flows in a channel. Examples differ in boundary and initial conditions and in used systems of equations.

Numerical Results of System 1. Isolines of velocity and pressure are shown in Fig. 5.3. Boundary conditions of this system (ABL) are no-slip conditions on the whole surface. Fig. 5.1 deals with residua of presented examples to show the convergence of used methods. Residuum belonging to the computation of the system 1 is presented in the middle part of Fig. 5.1.

Numerical Results of System 2. In Fig. 5.2 isolines of velocity and pressure are shown; boundary conditions for this case (channel) are no-slip conditions on the hill surface, free-slip conditions on the rest of surface.

As said earlier, in the case of computation of flows in a channel the density is computed. Figs. 5.4 and 5.5 demonstrate examples of the density perturbation $\rho' = \rho - \rho_B$ and the density ρ. Results in both figures differ in value of $\frac{\partial \rho_B}{\partial y}$. At the lower boundary, there is $\rho_B^L = 1$ in the both cases; in the first case, $\rho_B^U = 0,8$, and in the latter case, $\rho_B^U = 0,5$, at the upper boundary. ρ_B is an initial distribution of the density.

Fig. 5.1 deals with residua, as mentioned above. Both the first and the third residuum belong to the computation of the system 2 (channel). The first one is the residuum of the computation of flows in a channel with values $\rho_B^L = 1$ and $\rho_B^U = 0,8$; the last one shows the residuum belonging to flows in a channel with values $\rho_B^L = 1$ and $\rho_B^U = 0,5$.

5. Conclusion. A short description of computed problems - flow in the atmosphere and in a channel of finite depth - is presented in this paper, and the first achieved numerical results are discussed. All the important methods used for the computation are mentioned as well. In the future, results shown in this paper will be compared with next numerical results of the same problems obtained by different numerical methods.

Acknowledgement. Partial support of the project "Applied Mathematics in Physics and Technical Sciences", No. MSN6840770010 of the Ministry of Education, Youth and Sports of the Czech Republic is acknowledged.

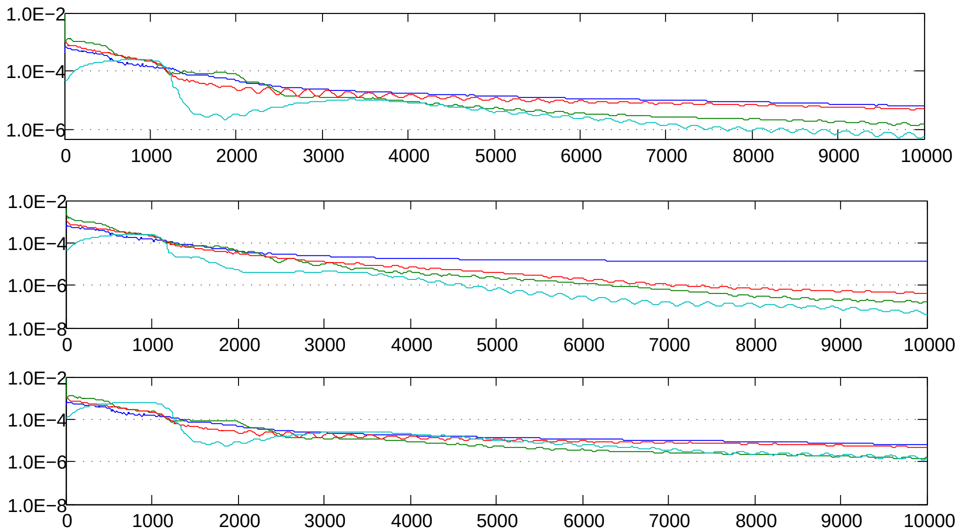

FIG. 5.1. *Residua. 1. Flows in a channel,* $\rho_B^L = 1$ *and* $\rho_B^U = 0.8$*. 2. Flows in the atmospherical boundary layer,* $\rho_B^L = 1$ *and* $\rho_B^U = 0.8$*. 3. Flows in a channel,* $\rho_B^L = 1$ *and* $\rho_B^U = 0.8$*.*

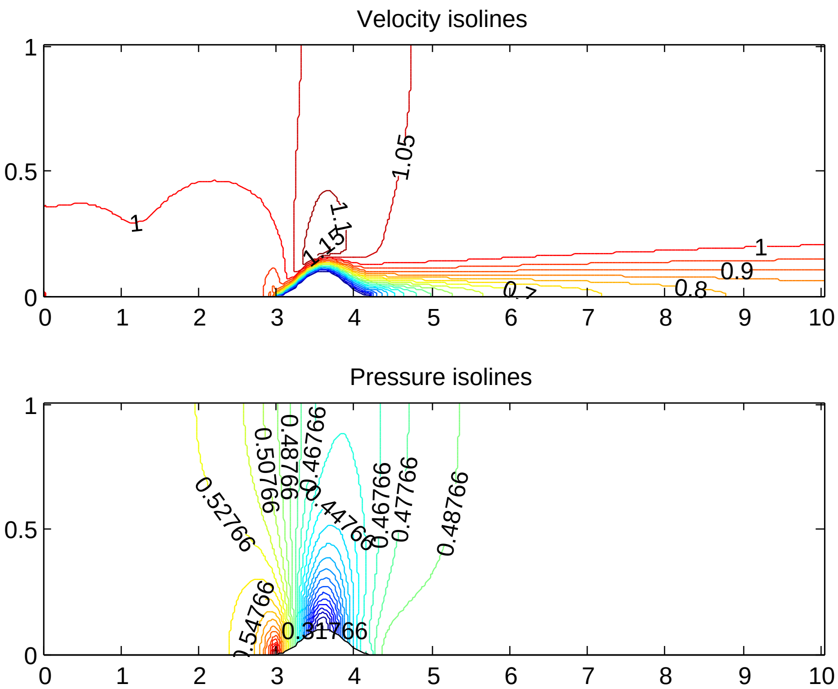

Fig. 5.2. *Model of a flow in a channel of finite depth. Isolines of velocity and pressure. No-slip conditions on the hill surface, free-slip conditions on the rest of surface. Re* = 2000, *number of iterations 10000.*

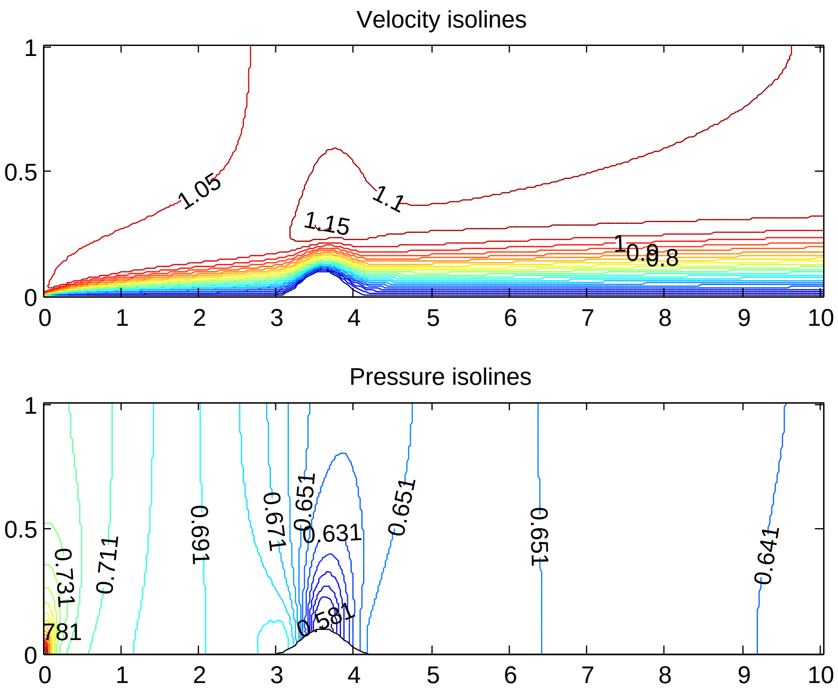

Fig. 5.3. *Model of a flow in the atmospheric boundary layer. Isolines of velocity and pressure. No-slip conditions on all the surface. Re* = 2000, *number of iterations 10000.*

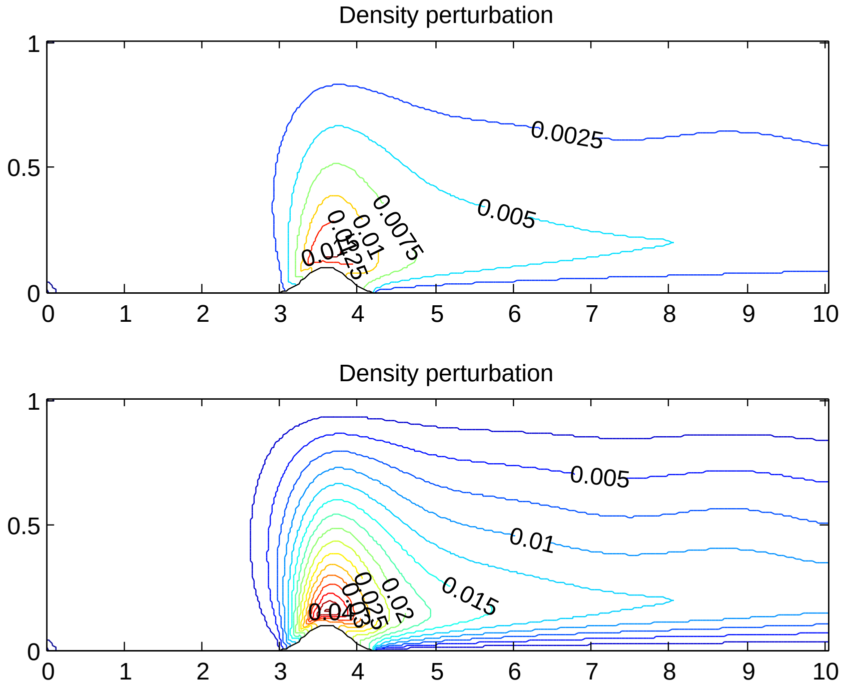

FIG. 5.4. *Model of a flow in a channel of finite depth. Isolines of density perturbation for. Upper figure* $\rho_B^L = 1$ *and* $\rho_B^U = 0.8$, *lower figure* $\rho_B^L = 1$ *and* $\rho_B^U = 0.5$. *Re* $= 2000$, *number of iterations 10000.*

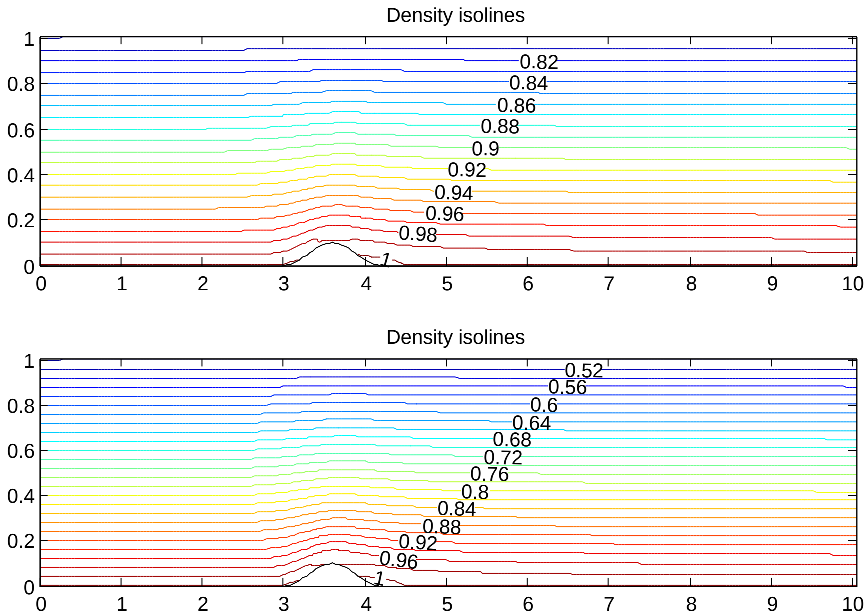

FIG. 5.5. *Model of a flow in a channel of finite depth. Isolines of density. Upper figure* $\rho_B^L = 1$ *and* $\rho_B^U = 0.8$, *lower figure* $\rho_B^L = 1$ *and* $\rho_B^U = 0.5$. *Re* $= 2000$, *number of iterations 10000.*

REFERENCES

[1] T. Uchida, and Y. Ohya, *Numerical study of stably stratified flows over a two-dimensional hill in a chanel of finite depth*, Fluid Dynamics Research, **29** (2001), 227–250.
[2] T. Uchida, and Y. Ohya, *Numerical simulation of atmospheric flow over complex terrain*, Journal of Wind Engineering and Industrial Aerodynamics, **81** (1999), 283–293.
[3] T. Bodnár, *Numerical Simulation of Flows and Pollution Dispersion in Atmospheric Boundary Layer*. Disertation Thesis, Czech Technical University in Prague (2003).
[4] K. Kozel, and R. Dvořák, *Mathematical Methods in Aerodynamics*. CTU Press, Prague, (1992), (in Czech).